Anisotropic Turbulent Heat Flux Modelling through Shock Waves

Subhajit Roy* and Krishnendu Sinha †
Indian Institute of Technology Bombay, India

Francis Lacombe‡ and Jean-Pierre Hickey §
University of Waterloo, Waterloo, Ontario, Canada

Classical approaches to model the turbulent heat flux rely on the gradient diffusion hypothesis which assumes an alignment between the temperature gradient and turbulent heat flux. This assumption is generally valid but breaks down in the vicinity of shocks. Particularly in shock-turbulence boundary layer interaction (STBLI), the anisotropy of the post-shock turbulence imparts an anisotropic heat flux to the wall that is not aligned with the mean thermal gradient. We derive a turbulent heat flux model that can be implemented into a Reynolds Stress Model (RSM). It models the turbulent heat flux with the information provided from the Reynolds stress components of RSM. The heat flux model is first validated against DNS of a planar shock turbulence interaction problem. Afterwards, the model is implemented into a full Navier-Stokes solver, CFL3D, in order to simulate a shock-boundary layer interaction problem.

I. Nomenclature

M	=	Mach number
c_p	=	Specific heat at constant pressure
ρ, p, T	=	density, pressure, and temperature
$(\Phi)'/(\Phi)''$	=	Reynolds/Favre fluctuations of variable Φ
$\overline{(\Phi)}/\widetilde{(\Phi)}$	=	Reynolds/Favre average of variable Φ
$(\Phi)_u$/ $(\Phi)_d$	=	upstream/ downstream quantities of variable Φ
μ, ν	=	kinematic and dynamic viscosity
μ_t, ν_t	=	kinematic and dynamic turbulent viscosity
Pr, Pr_T	=	Prandtl and turbulent Prandtl number
k	=	turbulent kinetic energy
ϵ	=	specific dissipation
C_μ, C_θ	=	model constants
ξ_t	=	mean position of the shock
b_1	=	closure coefficient
ϕ	=	estimator of flow compressibility
R_{ij}	=	Reynolds stresses

In high-speed flow applications, shock-turbulence boundary layer interactions (STBLI) are responsible for a localized peak in the wall heat transfer in the post-shock region. From an engineering perspective it is critical to accurately predict the location and magnitude of this peak thermal load as it dictates the parameters of the needed thermal protection system. The localized heating is directly tied to the mean flow pressure/temperature rise through the shock but–more importantly near solid walls–to the increased turbulent heat flux impinging on the surface. Whereas the mean flow properties through a shock are rather simple to predict, the turbulent heat flux remains more difficult to estimate as both the jumps in turbulent kinetic energy and thermal fluctuations through the shock must be accurately predicted.

*Ph.D. student, Department of Aerospace Engineering, Powai, Mumbai-400 076
†Professor, Department of Aerospace Engineering, Powai, Mumbai-400 076, and AIAA Member
‡Ph.D. student, Department of Mechanical and Mechatronics Engineering, 200 University Ave. W.
§Assistant Professor, Department of Mechanical and Mechatronics Engineering, 200 University Ave. W.

Furthermore, the strong anisotropy of the post-shock turbulence in STBLI results in a highly-directional turbulent heat flux. In other words, the modelling of the post-shock turbulence anisotropy is needed, at a minimum, to accurately capture the peak thermal loading in shock-wave boundary layer interactions. This anisotropic heat flux modelling in the context of Reynolds-Averaged Navier-Stokes (RANS) equations is the focus of the present work.

As the turbulent stresses are important contributors to the turbulent heat flux in the STBLI, classical, two-equation RANS turbulence models prove to be inadequate in determining the maximum surface heat loading. Although corrections may be applied to accurately capture the turbulent kinetic energy jump through the shock [1], the two-equation models are unable to provide quantitative estimates of the local turbulence anisotropy. Reynolds-stress equation-based models (RSM) resolve the full Reynolds stress tensor but require modifications to capture the changes to the off-diagonal terms when passing through a shock. Recent works have proposed different approaches to account for the Reynolds stresses increase in a shock-turbulence interaction [2, 3].

Despite the observable anisotropy of the turbulent heat flux, most existing RANS-based models rely on the gradient diffusion hypothesis (GDH) to relate the turbulent heat flux to the known turbulence quantities. The introduction of this model is often attributed to [4], although ideas had been presented prior. The typical GDH model–used for both two-equation and RSM–reads [5]:

$$c_p \overline{\rho u'' T''} \approx -\frac{c_p \mu_t}{Pr_t} \frac{\partial \overline{T}}{\partial x_j} \tag{1}$$

Despite the prevalence of this turbulence heat flux assumption, this model does not account for the anisotropy of the turbulent stress and only the turbulent kinetic energy is used in modelling the eddy viscosity term. Of note, some of the seminal works (see e.g. [6]) actually consider the individual Reynolds stress components before making a simplifying assumption of isotropic thermal diffusivity.

A further limitation of the above model lies in the use of the turbulent Prandtl number which is known to vary greatly across the shock [7]. The turbulent Prandtl number is often selected independently from the Mach number of the problem, thus greatly impacts the turbulent heat flux prediction in the post-shock region. The importance in defining a turbulent Prandtl number in hypersonic flows calculations was presented in [8].

The gradient diffusion hypothesis assumes that the maximum turbulent heat flux must be aligned with the maximum mean temperature gradient. This hypothesis has been questioned in very simple flows. Experimentally, it has been shown that the turbulent heat flux in the axial direction of a fully turbulent pipe is three times larger than in the wall normal direction [9, 10]. The under-prediction of the $\overline{u'T'}$ due to the gradient diffusion hypothesis has been observed in a number of simulations [11]. Other workers [12, 13] used a higher order turbulent heat flux model which decomposes the eddy diffusivity tensor into symmetric and anti-symmetric parts. This approach permitted improved predictions in a number of canonical turbulent heat transfer cases.

The gradient diffusion hypothesis has been questioned in [14] for supersonic flows. As the turbulent heat flux relies on the mean temperature gradient in GDH based models; it attains a zero value upstream and downstream of a shock wave due to the uniformity of mean temperature. Whereas, direct numerical simulation (DNS) data clearly shows a peak positive value of turbulent heat flux just downstream of the normal shock wave due to the generation of anisotropy across the shock wave. Quadros et al. [14] proposed an alternative formulation of turbulent heat flux based on linear interaction analysis (LIA) which improves the post-shock prediction of heat transfer for a given range of freestream Mach numbers. But, being a differential equation based model, it will invariably increase the computational cost of the simulation.

In the present work, we present a novel approach to model the anisotropic heat flux in shock-turbulence interaction (STI) and shock-turbulent boundary layer interaction (STBLI) problems. The proposed turbulent heat flux estimation is developed within the context of Reynolds stress model (RSM) without the reliance on GGHD. The model and modelling assumptions are presented in the following section. The application of the model to STI is done to assess the normal component of the turbulent flux, the results are presented in Section 3. The applicability of the model to more complex two dimensional flows is investigated in Section 4. To this end, the model is integrated into CFL3D and a STBLI problem is investigated. In Section 5, the conclusions are drawn.

II. Anisotropic turbulent heat flux modelling

The peak wall heating observed in shock-turbulence boundary layer interactions (STBLI) is very important to tackle from a design perspective. An inaccurate prediction of the location and magnitude of this wall heat flux leads to severe structural damage along with a reduction in vehicle performance. Reynolds averaged Navier-Stokes (RANS) turbulence models are often used to model the complex flow physics in STBLI, owing to their low computation cost.

The gradient diffusion hypothesis (GDH) and the Reynolds analogy are used to model the turbulent heat flux:

$$\overline{u'T'}_{\text{GDH}} = -\frac{\nu_T}{Pr_T}\frac{\partial \overline{T}}{\partial x}, \tag{2}$$

where ν_T is the turbulent kinematic viscosity. It is related to turbulent kinetic energy via the dissipation rate ϵ in the standard k-ϵ turbulence model.

$$\nu_T = C_\mu \frac{k^2}{\epsilon} \tag{3}$$

The strong Reynolds analogy relates the turbulent heat flux to the Reynolds stress (in terms of kinematic eddy viscosity ν_T) via a constant value of turbulent Prandtl number. The gradient diffusion hypothesis assumes isotropic turbulence and the heat flux vector is aligned with the corresponding mean temperature gradient. But this simple assumption breaks down in cases where the heat flux is not aligned with the mean temperature gradient, such as shock waves with highly anisotropic downstream flow. As a result, the GDH is known to inaccurately predict turbulent effects in such flows.

A more general rigorous approach was proposed by Daly and Harlow [4]. They modeled the turbulent thermal diffusivity, $\alpha_T = \frac{\kappa_T}{\overline{\rho} c_p}$ in terms of Reynolds stresses to account for the anisotropy.

$$\overline{u'T'}_{\text{GGDH}} = -C_\theta \frac{k}{\epsilon}\overline{u'^2}\frac{\partial \overline{T}}{\partial x} \tag{4}$$

Here $C_\theta = 0.3$ is a model constant, k is the turbulent kinetic energy and ϵ is the dissipation of turbulent kinetic energy. This model has been used for pipe and duct flows where it overcomes one of the shortcoming of GDH due to misalignment of the turbulent heat flux and mean temperature gradient but gives wrong results of heat flux in the normal direction to mean temperature gradient [15]. The above model is often known as general gradient diffusion hypothesis (GGDH).

Both models will give a peak negative value of turbulent heat flux at the shock wave whereas they will attain a zero value upstream and downstream of the shock. The models are also highly grid dependent because of the mean temperature gradient and they will increase the magnitude with grid-refinement (without temperature gradient clipping or limiters). The only difference between the two models lies in the peak magnitude of the turbulent heat flux such that

$$\frac{\overline{u'T'}_{\text{GDH}}}{\overline{u'T'}_{\text{GGDH}}} = \frac{C_\mu}{C_\theta}\frac{k}{Pr_T}\frac{1}{\overline{u'^2}} \tag{5}$$

Both models are unable to capture the downstream peak positive heat flux value observed in DNS data. In short, the current approaches to model the turbulent heat flux cannot give accurate prediction downstream of a shock wave where the flow is highly anisotropic.

Here, we consider a different approach to model the turbulent heat flux across a normal shock wave. We assume that the GDH assumption is valid upstream of the shock wave where the flow is almost isotropic and model the upstream turbulent heat flux vector defined as in Eq. (2). Downstream of the shock, where the turbulence is most anisotropic, the gradient diffusion hypothesis breaks down and we used the method prescribed by Roy et al. [7] to model the downstream heat flux vector. The conservation of total enthalpy is used to model the turbulent heat flux behind the shock wave. The shock wave undergoes unsteady motion in response to the fluctuations of the turbulent flow. The deviation of the shock from its mean position is taken as $\xi(y, z, t)$, such that the temporal derivative ξ_t represents the instantaneous shock speed in the streamwise direction, Figure (1). The total temperature in the shock reference frame is written as

$$T_0 = \overline{T} + T' + \frac{(\overline{u} + u' - \xi_t)^2 + v'^2 + w'^2}{2c_p} \tag{6}$$

Here, u,v,w are the velocity components, overbar represents mean flow quantity and primes denote turbulent fluctuations. Assuming the shock speed and fluctuations to be small compared to the jumps in the mean flow quantities across the shock, the linearized total temperature conservation across the shock is given as:

$$T'_u + \frac{\overline{u_u}u'_u}{c_p} = T'_d + \frac{\overline{u_d}u'_d}{c_p} + \frac{\xi_t}{c_p}(\overline{u_u} - \overline{u_d}), \tag{7}$$

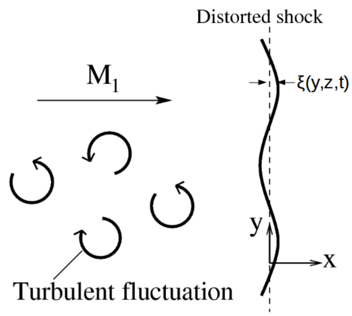

Fig. 1 Schematic of a distorted shock while interacting with upstream turbulent fluctuations

where the subscripts u and d denote the shock upstream and downstream location respectively. The left-hand side of the above equation represents the linearized form of the total temperature fluctuations upstream of the shock wave. We assume that the total temperature fluctuation in the upstream flow is negligible as per Morkovin's hypothesis [16] and the simplified form of the above equation is given as

$$T'_d + \frac{\overline{u_d} u'_d}{c_p} = -\frac{\xi_t}{c_p}(\overline{u_u} - \overline{u_d}) \tag{8}$$

which gives an expression for the turbulent heat flux behind the shock wave:

$$\overline{u'_d T'_d} = -\frac{\overline{u_d}}{c_p}\left(\overline{u'^2_d} + \overline{u'_d \xi_t}(r-1)\right) \tag{9}$$

where r is the mean density across the shock wave. Next, we employ the shock unsteadiness model of Sinha et al. [1], where the unclosed $\overline{u'_d \xi_t}$ correlation is written in terms of shock-normal Reynolds stress component:

$$\overline{u'_d \xi_t} = b_1 \overline{u'^2_d}, \quad \text{with} \quad b_1 = 0.4 + 0.6\left(\frac{6-r}{5}\right)^{5.2} \tag{10}$$

This is based on the assumption that the unsteady shock motion is caused by the incoming turbulent velocity fluctuations and the closure coefficient b_1 is obtained from linear interaction analysis. We thus get

$$\overline{u'_d T'_d} = -\frac{\overline{u_d}}{c_p} R_{11d}\left(1 + b_1(r-1)\right) \tag{11}$$

where $R_{11} = \overline{u'^2}$ is the shock-normal Reynolds stress. Similarly the expressions for $\overline{v'_d T'_d}$ and $\overline{w'_d T'_d}$ are

$$\overline{v'_d T'_d} = -\frac{\overline{u_d}}{c_p}\left(R_{12d}\right) \tag{12}$$

$$\overline{w'_d T'_d} = -\frac{\overline{u_d}}{c_p}\left(R_{13d}\right) \tag{13}$$

where $R_{12} = \overline{u'v'}$ and $R_{13} = \overline{u'w'}$. Clearly, across a normal shock these two terms will equal zero; but within a turbulent boundary-layer or sheared turbulence, these terms will have a finite value through a shock wave. In the above expressions, we also assume that

$$\overline{v'_2 \xi_t} = \overline{w'_2 \xi_t} \simeq 0, \tag{14}$$

i.e., the shock-speed has a very weak correlation with the transverse velocity fluctuations. Now the upstream components of turbulent heat flux vector are modeled as per gradient diffusion hypothesis, so we introduced a blending function $f(r)$

$$f(r) = \exp[1000(1-r)] \tag{15}$$

The value of $f(r) = 1$ in the upstream flow where $r = 1$ and $f(r) = 0$ in the downstream flow where r has a finite value. Thus the heat flux components are given as

$$\overline{u'T'} = -\frac{\overline{u}}{c_p} R_{11} \left(1 + b_1(r-1)\right) [1 - f(r)] - \frac{\mu_T c_p}{Pr_T} \frac{\partial \overline{T}}{\partial x} f(r) \tag{16}$$

$$\overline{v'T'} = -\frac{\overline{u}}{c_p} \left(R_{12}\right) [1 - f(r)] - \frac{\mu_T c_p}{Pr_T} \frac{\partial \overline{T}}{\partial y} f(r) \tag{17}$$

$$\overline{w'T'} = -\frac{\overline{u}}{c_p} \left(R_{13}\right) [1 - f(r)] - \frac{\mu_T c_p}{Pr_T} \frac{\partial \overline{T}}{\partial z} f(r) \tag{18}$$

The above models account for the local turbulence anisotropy downstream of the shock yet revert back to a classical GGDH model elsewhere. This local turbulence anisotropy is accounted for by incorporating the RSM terms of the Reynolds stress tensor.

III. Planar shock turbulence interaction (STI)

The Reynolds stress model (RSM) can be used to compute different component of turbulent heat flux vector across a shock wave. Also, the assumption of upstream negligible total temperature fluctuation needs to be modified for the canonical shock-turbulence interaction case. Most of the canonical STI problems consider purely vortical turbulence upstream and thus only $T'_u = 0$ in Eq. (6) and the contribution of u'_u needs to be retained in the derivation, which leads to a slightly different velocity-temperature correlation for STI problem:

$$\overline{u'_d T'_d} = \frac{\overline{u_d}}{c_p} R_{11d} \left(r\alpha - 1 - b_1(r-1)\right) \tag{19}$$

where the model parameter α relates the upstream and downstream velocity fluctuation; $\overline{u'_u u'_d} \sim \alpha \overline{u'^2_d}$. Here $\alpha = \max(0.6, \exp(0.25(1 - M_1)))$, note that for higher freestream Mach number ($M_1 \geq 3$) the value of $\alpha \rightarrow 0.6$, which is consistent with Roy *et al.* [7]. The value of $\alpha = 0.6$ gives a negative peak heat flux value at lower Mach number and we put a lower Mach number correction to avoid the negative peak heat flux. The value α is equal to 1 for sonic flow. Hence the heat flux equation for STI problem

$$\overline{u'T'} = \frac{\overline{u}}{c_p} R_{11} \left(r\alpha - 1 - b_1(r-1)\right) [1 - f(r)] - \frac{\mu_T c_p}{Pr_T} \frac{\partial \overline{T}}{\partial x} f(r) \tag{20}$$

We have solved the mean flow by one-dimensional inviscid Reynolds–averaged Navier–Stokes equations and the model prescribed by Babu and Sinha [3] is used to find the unclosed Reynolds stresses. The Lax-Friedrich scheme is used to evaluate the inviscid fluxes at the cell faces and the turbulence source terms are calculated at the cell centers. Although the first order accurate Lax-Friedrich method is highly dissipative in nature compared to other higher order schemes but it can match those higher order results by using a large number of points [17]. A much higher grid count can be used in these one-dimensional flows. A constant Courant–Friedrichs–Lewy (CFL) number of 0.4 is used for all the simulated results presented here.

Fig. 2 shows the model comparison with the DNS data of Larsson et al. [18] for a Mach number range of 1.5 to 6. The standard GDH model predicts a large negative value of the turbulent heat flux across a normal shock wave whereas the current model matches the DNS data for all the cases considered here. The center of the mean shock is located at $x/L_\epsilon = 0$ for all the cases and the vertical dashed lines represent the mean shock thickness. Note that, the mean shock-thickness reduces with increased free-stream Mach number. Here the velocity fluctuation is normalized by upstream mean velocity and the temperature fluctuation is normalized by downstream mean temperature. The correlation is further normalized by the upstream normalized turbulent kinetic energy. Also, the streamwise distance is normalized by the dissipation length scale L_ϵ.

IV. Shock-turbulence boundary layer interaction (STBLI)

For completeness, we integrate the turbulent heat flux model into a full Navier-Stokes solver and solve a well-defined shock-turbulence boundary-layer interaction (STBLI) problem. One of the relevant cases of study is the supersonic

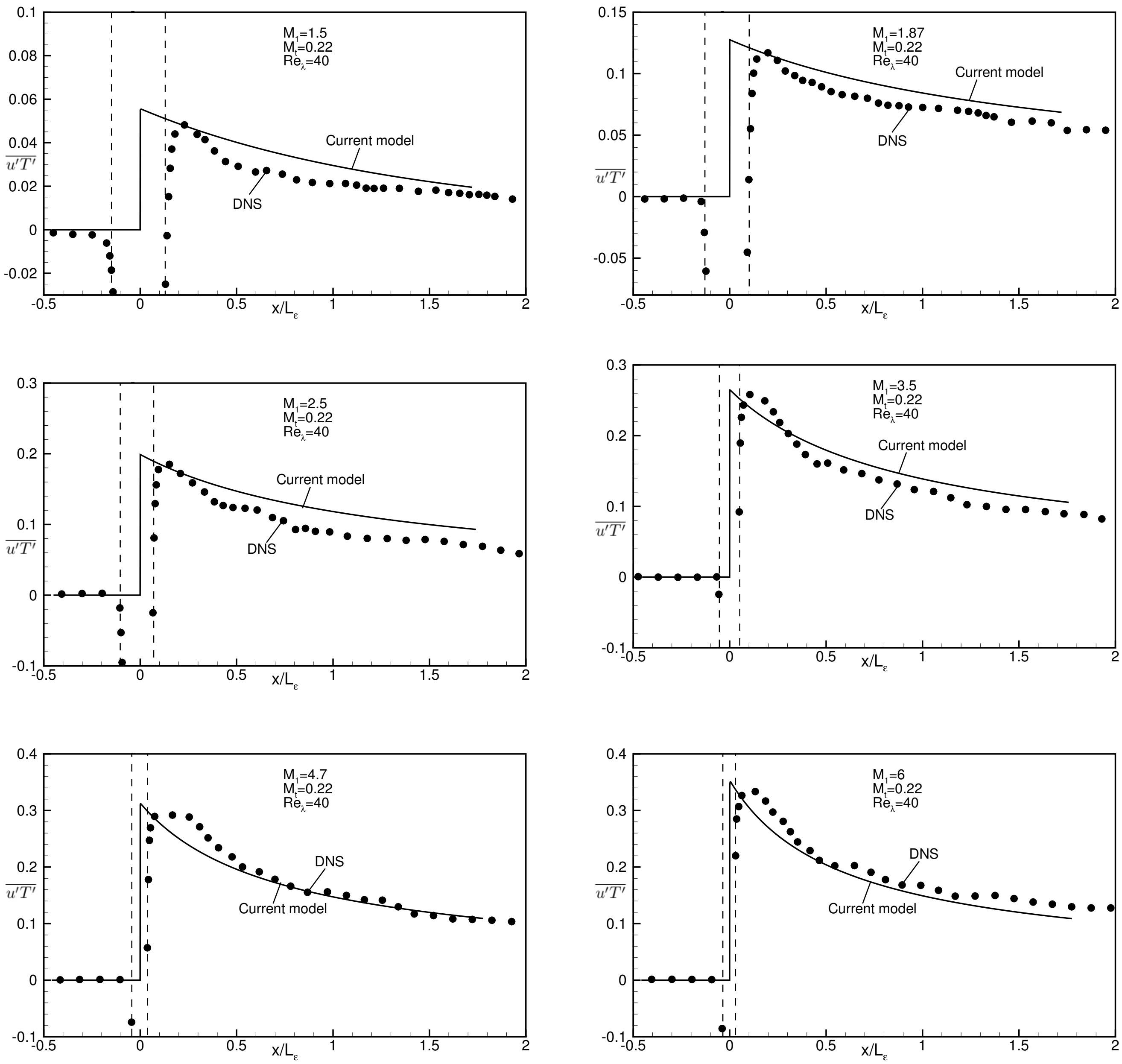

Fig. 2 Streamwise variation of $\overline{u'T'}$ for different freestream Mach numbers. The computed results are compared with the DNS data of Larsson et al. [18]

wedge compression corner [20], for which experimental data are available. In order to implement this model, we define a parameter to assess the proximity to the shock, r. This function is needed for the calculation of the blending function $f(r)$, is generally not straightforward to obtain without the implementation of an additional transport equation. To overcome this difficulty, we use an algebraic expression based on previous works of Sinha *et al.* [19] to locally compute the shock proximity. The flux equation for the STBLI problem is thus slightly different from the STI case. For instance, in the streamwise direction, the heat flux reads:

$$\overline{u'T'} = -\frac{\overline{u}}{c_p} R_{11}(1 + b_1(1 - \phi))(1 - f(\phi)) - \frac{\mu_T c_p}{Pr_T} \frac{\partial T}{\partial x} f(\phi) \tag{21}$$

$$\overline{v'T'} = -\frac{\overline{u}}{c_p} R_{12}(1 - f(\phi)) - \frac{\mu_T c_p}{Pr_T} \frac{\partial T}{\partial y} f(\phi) \tag{22}$$

$$\overline{w'T'} = -\frac{\overline{u}}{c_p} R_{13}(1 - f(\phi)) - \frac{\mu_T c_p}{Pr_T} \frac{\partial T}{\partial z} f(\phi) \tag{23}$$

where ϕ is given by equation (24), an estimator of the flow compressibility; $\phi = 0$ in high-compressibility regions and $\phi = 1$ otherwise. It is algebraically defined as

$$\phi = \frac{1}{2} \tanh\left(10 \frac{S_{ii}}{S + 500} + 3\right) - \frac{1}{2} \tag{24}$$

The anisotropic heat flux correction was implemented into CFL3D, an open-source, structured-grid Reynolds-averaged Navier-Stokes (RANS) code [21]. The code solves the compressible Navier-Stokes equations on a multi-block structured grid using standard second-order finite volume approximations. The solver speed greatly benefits from a multi-grid implementation. We use the well-documented SSG/LRR RSM turbulence model [22]; we make the modifications to the turbulent heat flux implementation of this RSM model and compare to the standard GGDH model.

For the STBLI test case, we consider a flat plate/wedge configuration with a 36° inclination as per in the report by [24]. The operating condition is set to a free-stream Mach number of 9.22 and Reynolds number of 26.2 million. The domain size is selected to study the compression corner shock turbulence interaction. All the simulations are fully wall-resolved using a fully structured, two-dimensional mesh with over 1.3 million cells ($975 \times 663 \times 2$). The geometrical configuration and additional experimental details can be found in [23],[26] and [25]. At these selected operating configurations, a separation region appears in the corner and a peak heat flux is observed on the ramp in the immediate post-shock region.

The overall organization of the shock structure remains almost unchanged with the integration of the new anisotropic heat transfer model in Figure 4 (a) and (b). This observation is consistent with the expected modest influence of the turbulent heat transfer on the general flow features. Furthermore, away from the shocks, we expect both heat transfer models to deliver identical results, as a result the differences arise only in the vicinity of the shock. A closer inspection of the near wall temperature field in figure 5 reveals some slight variations between both cases, although most of the variation is located away from the wall near the shock wave. Figures 7 show the wall normal profile of temperature and density at the location of the maximum heat flux. Both models provide a similar estimate of the near wall thermal layer although slight differences are observed at other locations in the profile. When comparing with experimental results, the normalized pressure distribution on the wall, in Figure 6 (b), is only very slightly impacted by the turbulent heat flux model. The corrected model produces a slightly longer separation region ($\approx 10\%$ longer) than the Generalized Gradient Diffusion Hypothesis (GGDH) and the surface heat flux is slightly reduced with the new model.

V. Conclusion

A model to account for the anisotropic turbulent heat transfer of supersonic flows with shock waves is developed. The model blends a newly developed algebraic model in the vicinity of the shock wave with standard gradient diffusion hypothesis away from the shock. The model is then assessed against classical cases of shock turbulence interaction (STI) and shock-turbulence boundary layer interaction (STBLI). The STI results shows good agreement in both the peak value and decay of the turbulent heat flux. The STI cases presented here only considered a single turbulent Mach number (M_t) and Reynolds number based on Taylor micro scale (Re_λ). The generalizability of the model to account for a greater range M_t and Re_λ values will be left for future work. The model was also implemented into a compressible Computational Fluid Dynamic solver, CFL3D. More specifically, the turbulenct heat transfer model was integrated into the existing SSG/LRR framework for the RSM turbulence model. The CFD framework was used to study the more

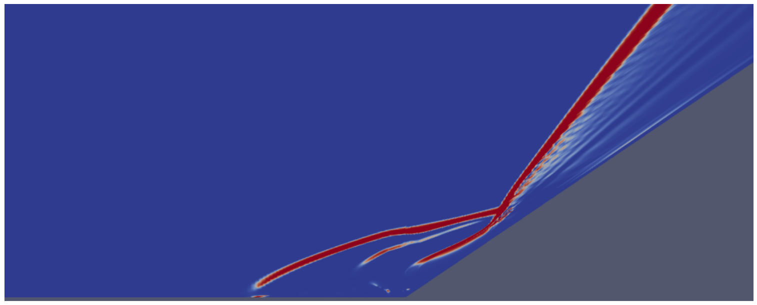

Fig. 3 Compressibility indicator ϕ for the case of the hypersonic wedge flow

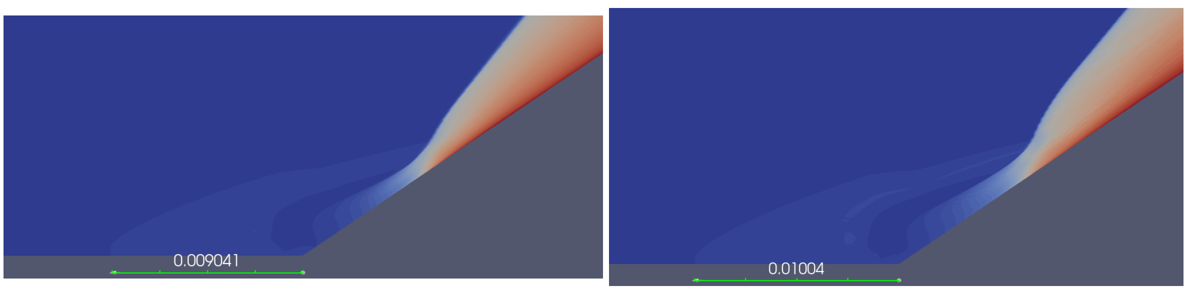

(a) **(b)**

Fig. 4 Qualitative comparison of the pressure distribution using the GGDH (a) and the newly implemented model (b). The color scales of the respective figures are identical.

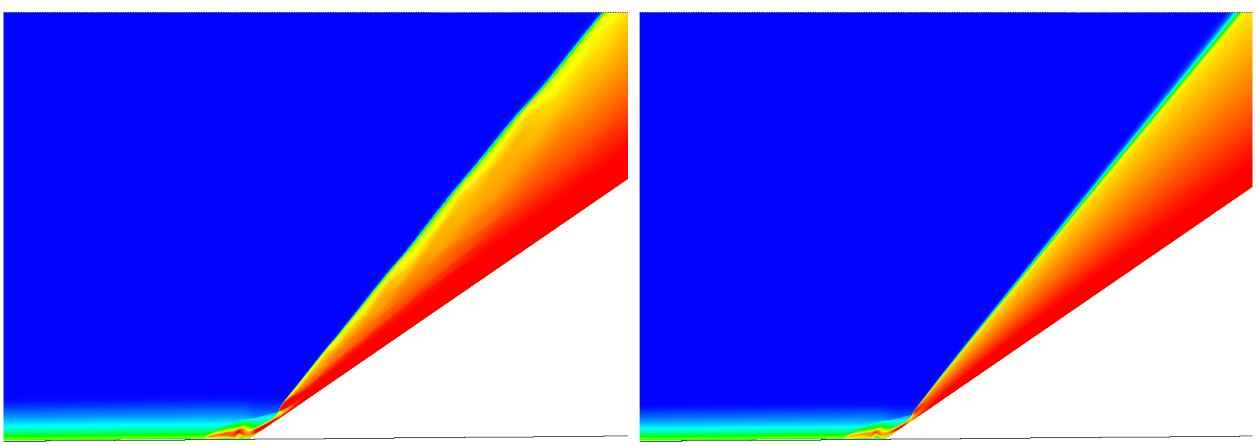

Fig. 5 Temperature color plot (identical scale) for the GGDH (left) and corrected heat flux model (right).

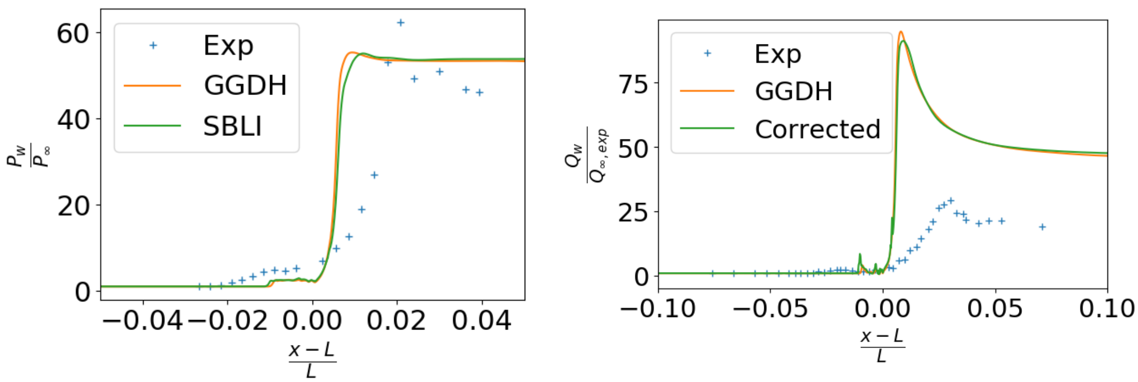

(a) **(b)**

Fig. 6 Normalized wall pressure (P/P_∞) and surface heat transfer($Q_w/Q_{,exp}$)

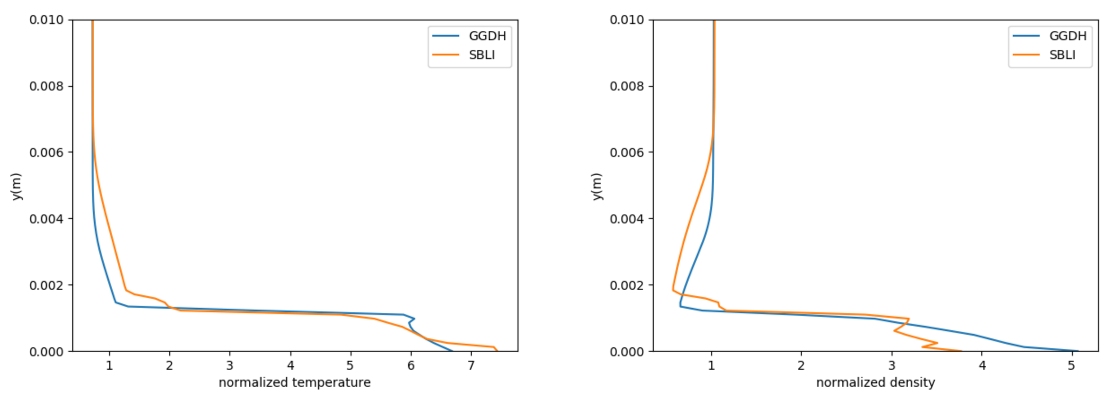

(a) **(b)**

Fig. 7 Temperature (a) and density (b) profiles normal to the ramps at the location of maximum heat transfer.

complex setup of STBLI, generated from a planar wedge, in which the mean temperature gradient and turbulent heat flux are not aligned. In the STBLI, the anisotropy of the post-shock turbulence imparts an anisotropic heat flux to the wall. Although the present CFD results are fully grid converged, the numerical results do not capture the correct separation bubble in the compression corner and present a slight departure from the experimental data. Nonetheless, the integral flow structures (shock position, wall pressure distribution etc.) remain unaffected by the turbulent heat flux model while the turbulent heat flux at the wall is reduced with the new model and shows a better agreement.

Acknowledgments

The project is partially supported by Shastri Indo-Canadian Institute and with the assistance of the Government of Canada. FL would like to acknowledge support by the NSERC PGS-D Grant.

References

[1] Sinha, K., Mahesh K., and Candler, G.V., "Modeling shock unsteadiness in shock/turbulence interaction," *Physics of Fluids*, Vol. 15, No. 8, 2003, pp. 2290-2297. doi: 10.1063/1.1588306

[2] Karl, S., Hickey, J.-P., and Lacombe, F., "Reynolds Stress Models for Shock - Turbulence Interaction," *International Symposium on Shock Waves*, Nagoya, Japan, 2017, p. 6.

[3] Babu, V. J., and Sinha, K., "Reynolds stress models applied to canonical shock-turbulence interaction," *Journal of Turbulence*, Vol. 18, No. 7, 2017, pp. 653-687. doi:10.1080/14685248.2017.1317923.

[4] Daly, B. J., and Harlow, F. H., "Transport equations in turbulence," *Physics of Fluids*, Vol. 13, No. 11, 1970, pp. 2634-2649. doi:10.1063/1.1692845.

[5] Wilcox, D., *Turbulence modeling for CFD*, 2nd ed., DCW industries La Canada, CA, 1998.

[6] Launder, B. E., "On the Computation of Convective Heat Transfer in Complex Turbulent Flows," *Journal of Heat Transfer*, Vol. 110, No. 4b, 1988, p. 1112. doi:10.1115/1.3250614.

[7] Roy, S., Pathak, U. and Sinha, K., "Variable Turbulent Prandtl Number Model for Shock/Boundary-Layer Interaction," *AIAA Journal*, , Vol. 56, No. 1, 2018, pp. 342-355. doi:10.2514/1.J056183.

[8] Xiao, X., Edwards J. R., Hassan A. H., and Gaffney R. L., "Role of turbulent Prandtl numbers on heat flux at hypersonic Mach numbers," *AIAA Journal*, Vol. 45, No. 4, 2007, pp. 806-813. doi: 10.2514/1.21447.

[9] Bremhorst, K., and Bullock, K., "Spectral measurements of temperature and longitudinal velocity fluctuations in fully developed pipe flow," *International Journal of Heat and Mass Transfer*, Vol. 13, 1970, pp. 1313-1329. doi:10.1016/0017-9310(70)90072-4.

[10] Sesonske, A., "*Turbulent Structure of Isothermal and Nonisothermal Vp1 I,*" Vol. 17, No. I, 1974, pp. 113-123.

[11] Schneider, H., Von Terzi, D. A., Bauer, H. J., and Rodi, W., "Coherent structures in trailing-edge cooling and the challenge for turbulent heat transfer modelling," *International Journal of Heat and Fluid Flow*, Vol. 51, 2015, pp. 110-119. doi: 10.1016/j.ijheatfluidflow.2014.10.013.

[12] Suga, K., and Abe, K., "Nonlinear eddy viscosity modelling for turbulence and heat transfer near wall and shear-free boundaries," *International Journal of Heat and Fluid Flow*, Vol. 21, No. 1, 2000, pp. 37-48. doi:10.1016/S0142-727X(99)00060-0.

[13] Suga, K., "Predicting turbulence and heat transfer in 3-D curved ducts by near-wall second moment closures," *International Journal of Heat and Mass Transfer*, Vol. 46, No. 1, 2003, pp. 161-173. doi:10.1016/S0017-9310(02)00249-1.

[14] Quadros, R. and Sinha, K., " Modelling of turbulent energy flux in canonical shock-turbulence interaction," *International Journal of Heat and Fluid Flow*, Vol. 61, 2016, pp. 626-635. doi: 10.1016/j.ijheatfluidflow.2016.07.006.

[15] Younis, B. A., Charles G. S., and Timothy T. C., "A rational model for the turbulent scalar fluxes," *Proceedings of the Royal Society of London A: Mathematical, Physical and Engineering Sciences*, vol. 461, No. 2054, The Royal Society, 2005, pp. 575-594. doi:10.1098/rspa.2004.1380.

[16] Morkovin, M. V., "Effects of compressibility on turbulent flows," *Mecanique de la Turbulence*, edited by Favre, A., Gordon and Breach, New York, 1964, pp. 367-380.

[17] Raje, P., and Sinha, K., “A physically consistent and numerically robust k-ϵ model for computing turbulent flows with shock waves,” *Computers & Fluids*, Vol. 136, 2016, pp. 35-47. doi: 10.1016/j.compfluid.2016.05.026.

[18] Larsson, J., and Lele, S. K., “Direct numerical simulation of canonical shock/turbulence interaction,” *Physics of Fluids*, Vol. 21, No. 12, 2009, p. 126101. doi:10.1063/1.3275856.

[19] Sinha, Krishnendu and Mahesh, Krishnan and Candler, Graham V., ”Modeling the Effect of Shock Unsteadiness in Shock/ Turbulent Boundary-Layer Interactions”, *AIAA Journal*, Vol. 43, 2005, pp. 586-594. doi: 10.2514/1.8611

[20] Holden, Michael S. and Wadhams, Tim P. and MacLean, Matthew G., ”Measurements in Regions of Shock Wave/Turbulent Boundary Layer Interaction from Mach 4 to 10 for Open and “Blind” Code Evaluation/Validation”, *21st AIAA Computational Fluid Dynamics Conference*, 2013 doi:10.2514/6.2013-2836

[21] Krist, S. L., Biedron, R. T., and Rumsey, C. L., CFL3D user’s manual: Version 5.0. Hampton, Va: National Aeronautics and Space Administration, Langley Research Center., 1998

[22] Eisfeld, B., Rumsey, C. and Togiti, V., Verification and validation of a second-moment-closure model, *AIAA Journal*, Vol. 54 (5), 2016, pp. 1524–1541. doi: 10.2514/1.J054718

[23] Elfstrom, G.M., Turbulent hypersonic flow at a wedge-compression corner, Journal of Fluid Mechanics, Vol. 53, part 1, 1972, pp. 113-127.

[24] Marvin, J., Brown, J., Gnoffo, P., Experimental database with baseline CFD Solutions: 2D and axisymmetric hypersonic shock-wave/turbulent boundary layer interactions, NASA TM-2013-216604, 2013.

[25] Coleman, G.T., Hypersonic Turbulent Boundary Layer Studies, PhD Thesis, Department of Aeronautics, Univ. of London, 1973.

[26] Coleman, G.T. and Stollery, J.L., Heat transfer from hypersonic turbulent flow at a wedge compression corner, Journal of Fluid Mechanics, Vol. 56, part 4, 1972, pp. 741-752.